NON-LTE ABUNDANCES AND CONSEQUENCES FOR THE EVOLUTION OF THE α-ELEMENTS IN THE GALAXY

T. IDIART AND F. THÉVENIN

Universidade de São Paulo, Instituto Astronomico e Geofisico, Departamento de Astronomia Avenida Miguel Stefano 4200,
São Paulo 01065-970, Brazil; thais@iagusp.usp.br; Observatoire de la Côte d'Azur B.P. 4229,
06304 Nice Cedex 4, France; thevenin@obs-nice.fr

ABSTRACT

Abundances of α-elements such as Ca and Mg in disk and halo stars are usually derived from equivalent width lines measured on high-resolution spectra and assuming local thermodynamic equilibrium (LTE). In this paper, we present non-LTE differential abundances derived by computing the statistical equilibrium of Ca I and Mg I atoms, using high-resolution equivalent widths available in the literature for 252 dwarf to subgiant stars. These non-LTE abundances, combined with recent determination of non-LTE abundances of iron, seem to remove the dispersion of the [Ca/Fe] and [Mg/Fe] ratios in the galactic halo and disk phases, revealing new and surprising structures. These results have important consequences for chemical evolution models of the Galaxy. In addition, non-LTE abundance ratios for stars belonging to the M92 cluster apparently have the same behavior. More high-resolution observations, mainly of globular clusters, are urgently needed to confirm our results.

Subject headings: Galaxy: abundances — radiative transfer — stars: abundances — stars: atmospheres

1. INTRODUCTION

The determination of abundances of nuclear species at distinct locations in the Galaxy (e.g., halo, disk, and bulge) comes mainly from the spectra of late-type star atmospheres. Measured abundances in cool stars at different stages of evolution give not only an understanding of stellar nucleosynthesis but also provide valuable information about the process of chemical enrichment of the Galaxy.

The archaeological tracers of the chemical evolution of a star system are the elements produced by explosive nucleosynthesis in Type II (SN II) and Type Ia (SN Ia) supernova events. The interest in using such elements as tracers rests on the fact that SN II and SN Ia progenitors have different lifetimes; SN II is the final stage in the evolution of massive stars, and SN Ia is a possible final result of the evolution of a close binary system of intermediate-mass stars. SNe II contribute to the enrichment of the interstellar medium (ISM) mainly with elements produced by the capture of α-particles (α-elements) and from the r-process, and SNe Ia produce elements belonging to the Fe peak. Consequently, the basic tools to constrain the evolution of ISM in the Galaxy are usually the analysis of relations between ratios of heavy elements [element/Fe] and Fe abundance [Fe/H].[1]

A first glance at the temporal behavior of α-elements shows that the ratio [α/Fe] is approximately constant for halo metal-poor stars ([Fe/H] $\leq$ −1.5) and decreases for metal-rich stars ([Fe/H] $>$ −1.5) belonging to the disk. This is reasonably explained by the chemical evolutionary models that assume progressive enrichment of the ISM by supernovae: the first generation of stars has in its atmospheres the signature of SN II events only (called the halo phase of the Galaxy), and the subsequent generations have signatures of both SN II and SN Ia events (disk phase).

However, a more precise analysis of [α/Fe] versus [Fe/H] shows a pronounced scatter, mainly in the region of metal-poor stars. This scatter has been interpreted mostly as a consequence of the inhomogeneity of the matter making up the stars rather than a result of poor observational data (Audouze & Silk 1995).

The derivation of abundances based on the analysis of high-resolution stellar spectra is usually made under the assumption of local thermodynamical equilibrium (LTE). In the last 15 years, many efforts to estimate errors on abundance determinations caused by LTE assumption have been made. Recent results for Ba II (Gigas 1986, 1988; Mashonkina & Bikmaev 1996), Sr II (Belyakova & Mashonkina 1997), Na I (Mashonkina, Sakhibullin, & Shimanskii 1993), Mg I (Gigas 1986; Mashonkina, Shimanskaya, & Sakhibullin 1996), Ca I (Drake 1991), B I (Kiselman & Carlsson 1996), Al I (Baumuller & Gehren 1997), Fe I and Fe II (Thévenin & Idiart 1999, hereafter TI99), O I (Mishenina et al. 2000), and Mg I (Zhao, Butler, & Gehren 1998) demonstrate that most lines can form far from LTE conditions. Thus, some important questions arise: what is the influence of non-LTE abundance calculations on the chemical evolution diagrams of the Galaxy? Do these computations add additional different constraints to the chemical history of enrichment of the matter in the Galaxy?

In this work, we present non-LTE abundances derived from the computation of statistical equilibrium of Ca and Mg atoms, using published equivalent widths (§ 3). The atomic data and stellar atmospheric models used are presented in § 2. α-elements such as Mg and Ca have well-known enhanced abundances in atmospheres of F–G metal-poor dwarf stars as a result of cumulative stellar generations. Recently, Nissen & Schuster (1997) and Jehin et al. (1999) proposed the existence of two sequences of stars having two different [α/Fe] ratios for intermediate stars ([Fe/H] $\approx$ −1). Their works are based on highly accurate observations of stars having approximately the same tem-

---

[1] [Fe/H] = log (N_{Fe}/N_H) − log $(N_{Fe}/N_H)_\odot$.

peratures and surface gravities. Based on our non-LTE computations, we found different branches or sub-populations of stars not only for intermediate metallicities; consequences for chemical evolution models of the Galaxy are presented in § 4. We draw our conclusions in § 5.

2. ATOMIC DATA AND STELLAR ATMOSPHERIC MODELS

The code we used to solve the equations of statistical equilibrium and radiative transfer is version 2.2 (1995) of MULTI (Carlsson 1986). This code allows us to obtain theoretical spectra of Mg I and Ca I for given stellar atmospheric models and atomic data.

The atomic models used are shown by Grotrian diagrams presented in Figures 1 and 2, for Mg I and Ca I, respectively. We included all the fine-structure levels of Mg I below 6 eV: 103 levels + continuum and 980 radiative transitions. For calcium, the model has 83 levels + continuum and 483 radiative transitions. We used the atomic energy level tables given by Hirata & Horaguchi (1995, hereafter HH95) and Martin et al. (1985). Oscillator strengths are from HH95, Kurucz (1993), and Thévenin (1989, 1990). We followed the procedure described in TI99 for the remaining atomic data: radiative and collisional damping coefficients, excitation, and ionization collisional cross sections. Photoionization cross sections are from TopBase. The van der Waals damping for all Mg lines was calculated using the approximation given by Unsöld (1955) and multiplied by a factor 1.3 as in TI99. For Ca we followed Cayrel et al. (1996). Note that the factor 1.3 is important only for strong saturated lines. As will be seen in § 3, we always tried to use lines lying on the linear part of the curve of growth, where this factor does not play an important role.

FIG. 2.—Level and Grotrian diagrams of Mg I atom
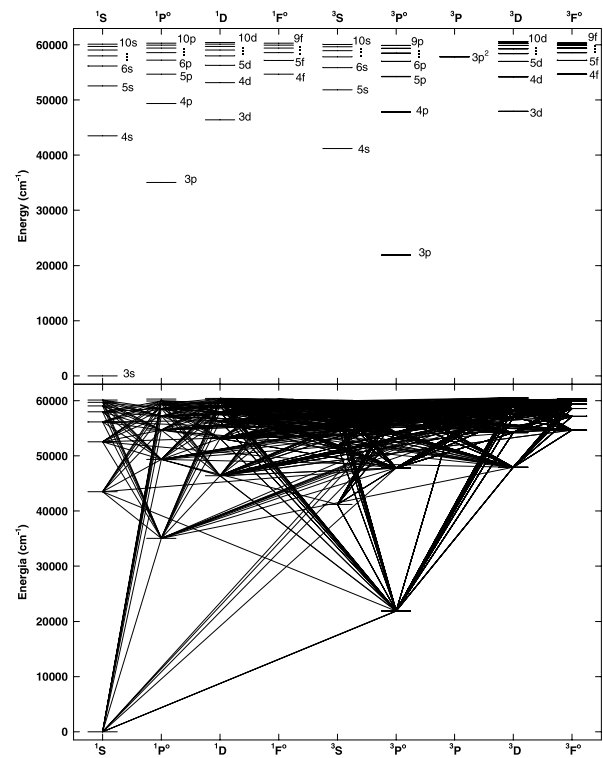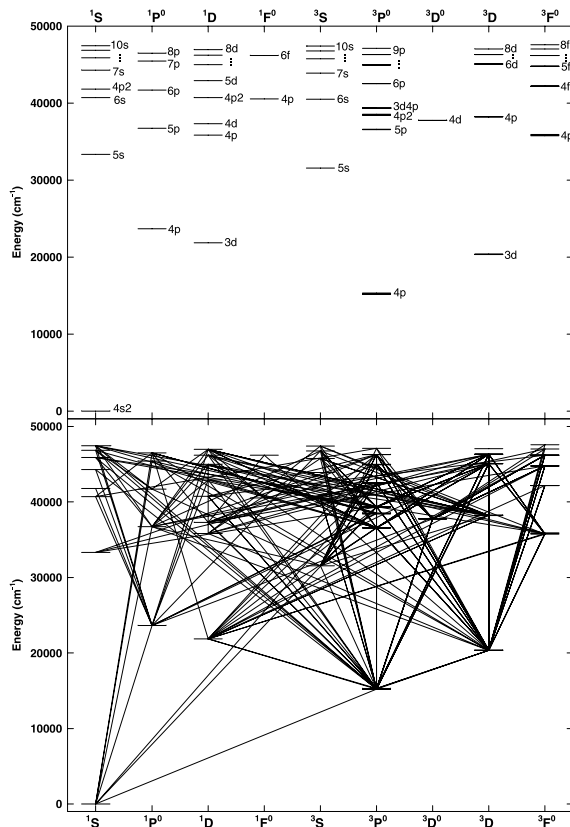

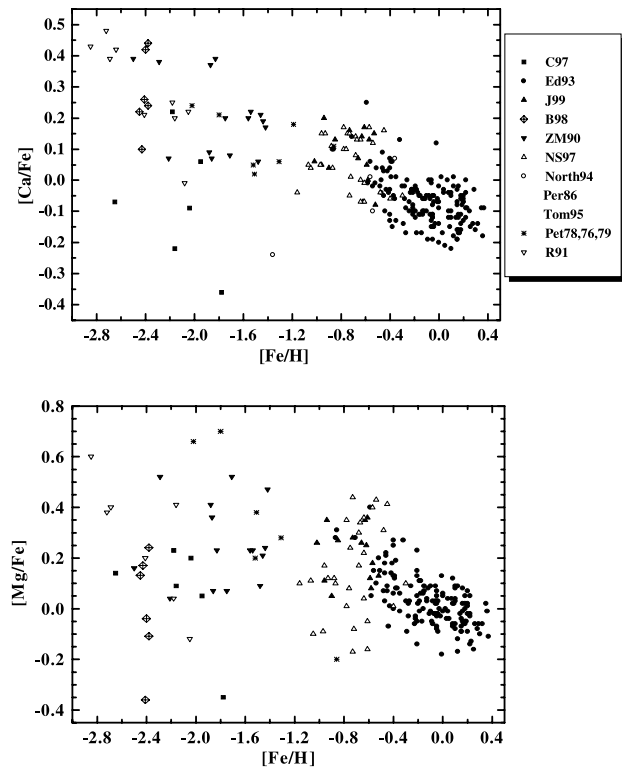FIG. 1.—Level and Grotrian diagrams of Ca I atom

FIG. 3.—Chemical evolution diagrams for non-LTE Ca I and Mg I abundances estimated in this work and non-LTE [Fe/H] by TI99. Distinct symbols refer to EW sources indicated by the legend above. North et al. (1994), Perrin (1986), and Tomkin, Lambert, & Balachandran (1985) are represented with the same symbols (*open circles*).

TABLE 1

ADDITIONAL AND REESTIMATED ATMOSPHERIC PARAMETERS
(COMPLEMENT OF TABLE 1 OF TI99)

Star	θ_{eff}	$\log g_{NLTE}$	$[Fe/H]_{NLTE}$
HD 3158	0.790	4.20	0.08
HD 3268	0.820	4.10	−0.13
HD 3567	0.827	4.20	−1.05
HD 4307	0.890	3.90	−0.17
HD 5015	0.810	4.10	0.10
HD 6582	0.950	4.67	−0.56
HD 6920	0.870	3.90	−0.05
HD 7476	0.770	4.15	−0.09
HD 7570	0.830	4.30	0.18
HD 9562	0.870	3.80	0.20
HD 9826	0.830	4.00	0.08
HD 10307	0.850	4.40	0.08
HD 12042	0.810	4.20	−0.22
HD 14214	0.830	4.10	0.15
HD 15335	0.860	4.20	−0.08
HD 15798	0.780	3.95	−0.10
HD 16673	0.800	4.40	0.10
HD 17288	0.882	4.32	−0.75
HD 17820	0.868	4.21	−0.54
HD 19994	0.830	4.10	0.18
HD 20807	0.840	4.50	−0.05
HD 22001	0.740	4.10	−0.01
HD 22484	0.840	4.20	0.00
HD 22879	0.861	4.35	−0.67
HD 23754	0.750	4.10	0.16
HD 24339	0.854	4.31	−0.48
HD 25621	0.800	4.00	0.16
HD 25704	0.856	4.35	−0.68
HD 26491	0.880	4.20	−0.08
HD 29645	0.840	4.10	0.16
HD 30562	0.860	4.00	0.22
HD 30743	0.780	4.20	−0.21
HD 33256	0.780	4.00	−0.14
HD 33608	0.760	4.10	0.37
HD 34411	0.860	4.10	0.09
HD 35296	0.790	4.30	0.10
HD 38393	0.790	4.30	0.00
HD 41330	0.850	4.10	−0.07
HD 43042	0.770	4.30	0.12
HD 43318	0.790	4.10	−0.03
HD 45701	0.870	4.20	0.20
HD 49933	0.760	4.20	−0.27
HD 50223	0.760	4.10	−0.04
HD 55575	0.850	4.00	−0.21
HD 59984	0.860	4.02	−0.62
HD 60532	0.820	3.92	−0.07
HD 61902	0.832	4.11	−0.59
HD 63077	0.880	4.33	−0.66
HD 63598	0.872	4.15	−0.73
HD 67228	0.870	4.20	0.14
HD 68456	0.770	4.10	−0.15
HD 70110	0.850	4.40	0.12
HD 76151	0.880	4.50	0.10
HD 78747	0.888	4.02	−0.61
HD 76932	0.860	3.75	−0.73
HD 79028	0.860	4.20	0.00
HD 79601	0.882	4.01	−0.53
HD 83220	0.777	4.20	−0.40
HD 86728	0.880	4.00	0.20
HD 87141	0.790	4.20	0.15
HD 88737	0.820	4.10	0.26
HD 88986	0.870	4.00	0.04
HD 89125	0.820	4.30	−0.24
HD 89744	0.800	4.10	0.28
HD 91752	0.780	3.90	−0.13

TABLE 1—Continued

Star	θ_{eff}	$\log g_{NLTE}$	$[Fe/H]_{NLTE}$
HD 91889	0.820	4.20	−0.11
HD 95128	0.860	4.30	0.04
HD 95241	0.860	4.10	−0.16
HD 97320	0.840	4.32	−1.02
HD 98991	0.760	4.00	0.00
HD 99747	0.760	4.00	−0.36
HD 102574	0.830	4.00	0.22
HD 102634	0.790	4.20	0.30
HD 102870	0.830	4.20	0.22
HD 103723	0.836	4.28	−0.61
HD 105004	0.864	4.28	−0.64
HD 106038	0.834	4.37	−1.07
HD 106516	0.804	4.37	−0.52
HD 107213	0.790	4.10	0.36
HD 108309	0.870	4.20	0.15
HD 108954	0.830	4.40	0.00
HD 109358	0.850	4.40	−0.05
HD 111971	0.857	4.21	−0.58
HD 112164	0.850	4.00	0.32
HD 113083a	0.859	4.42	−0.78
HD 113083b	0.874	4.42	−0.76
HD 113679	0.881	4.16	−0.45
HD 114642	0.790	3.90	−0.05
HD 114710	0.840	4.40	0.15
HD 115383	0.840	4.10	0.12
HD 115617	0.900	4.50	0.02
HD 120559	0.934	4.37	−0.78
HD 121004	0.886	4.41	−0.57
HD 121370	0.830	3.80	0.35
HD 124570	0.810	4.20	0.17
HD 124850	0.810	4.20	−0.05
HD 125184	0.910	3.90	0.23
HD 126681	0.900	4.37	−0.96
HD 126793	0.871	4.10	−0.63
HD 127334	0.900	4.00	0.16
HD 128167	0.750	4.40	−0.29
HD 128620	0.880	4.20	0.20
HD 131117	0.840	4.10	0.22
HD 136064	0.820	4.10	0.10
HD 136351	0.790	4.00	0.10
HD 137052	0.790	4.00	−0.05
HD 141004	0.850	4.00	−0.01
HD 142860	0.800	4.00	−0.06
HD 143761	0.780	4.40	−0.12
HD 144585	0.860	4.00	0.29
HD 151769	0.780	3.80	0.15
HD 152924	0.822	4.05	−0.57
HD 153597	0.800	4.40	−0.04
HD 156098	0.780	3.90	0.19
HD 159332	0.800	3.90	−0.06
HD 160032	0.760	4.10	−0.16
HD 163989	0.820	3.90	−0.05
HD 165908	0.840	4.35	−0.40
HD 168151	0.770	4.15	−0.19
HD 169830	0.790	4.20	0.20
HD 173667	0.800	4.20	−0.06
HD 175317	0.760	3.20	0.25
HD 177565	0.900	4.20	0.07
HD 181096	0.800	4.20	−0.13
HD 187013	0.810	4.00	−0.06
HD 187691	0.820	4.40	0.18
HD 189558	0.895	4.11	−0.94
HD 193901	0.883	4.69	−0.90
HD 194598	0.851	4.50	−0.96
HD 196378	0.830	4.20	−0.30
HD 196892	0.850	4.28	−0.85
HD 199289	0.867	4.40	−0.89

TABLE 1—*Continued*

Star	θ_{eff}	log g_{NLTE}	[Fe/H]$_{\text{NLTE}}$
HD 199623	0.800	4.20	−0.21
HD 200790	0.820	4.10	0.03
HD 203608	0.824	4.51	−0.52
HD 210855	0.810	3.90	0.18
HD 213657	0.830	3.94	−1.75
HD 215257	0.873	4.01	−0.67
HD 216385	0.820	4.10	−0.18
HD 217014	0.870	4.20	0.16
HD 218470	0.770	4.20	−0.04
HD 241253	0.854	4.45	−0.87
BD +20 3603	0.840	4.30	−2.04
BD +80 245	0.933	3.70	−1.78
BD −21 3420	0.848	4.31	−0.88
CD −33 3337	0.850	4.02	−1.16
CD −45 3283	0.890	4.58	−0.72
CD −47 1087	0.879	4.33	−0.64
CD −57 1633	0.850	4.30	−0.73
CD −61 0282	0.853	4.45	−0.97
G005 −040	0.859	4.22	−0.68
G046-031	0.837	4.43	−0.61
G088-040	0.845	4.18	−0.64
G90-3	0.876	4.28	−1.95
G102-020	0.935	4.50	−0.93
G125-64	0.892	5.45	−2.16
G190-15	1.008	5.20	−2.65
G182-31	0.840	4.38	−2.18
W7547	0.804	3.99	−0.30
M92-18	0.845	4.33	−2.45
M92-21	0.848	4.29	−2.38
M92-34	0.864	4.18	−2.43
M92-46	0.846	4.23	−2.41
M92-60	0.831	4.33	−2.40
M92-350	0.851	4.28	−2.38

FIG. 4.—Percentage error ϵ on Ca I and Mg I logarithmic abundances in function of atmospheric parameter variation for different lines of a star with $\theta_{\text{eff}} = 0.85$, log $g = 4.2$, and [Fe/H] = −2.0. These lines were used for abundance estimates of metal-poor stars (see Table 2). The variation of atmospheric parameters T_{eff}, log g, and [Fe/H] adopted here are the classical LTE errors and are on each corresponding diagram. Circles and upward- and downward-pointing triangles represent, respectively, [Ca/Fe] = +0.1, +0.25, and +0.45 and [Mg/Fe] = +0.6, +0.16, and −0.17.

Stellar atmospheric models are generated using the grids of Gustafsson et al. (1975) and Bell et al. (1976), in order to be consistent with TI99, using T_{eff} from Thévenin (1998) and log g and [Fe/H] corrected for non-LTE effects from TI99. We also estimated non-LTE log g and [Fe/H] values for an additional sample of stars not analyzed in TI99 (see Table 1). For some objects, for which more accurate equivalent widths were recently available, non-LTE surface gravities and [Fe/H] were reestimated (see Table 1). We emphasize that we do not intend to obtain absolute abundance values (see § 3); thus in a first approximation we can
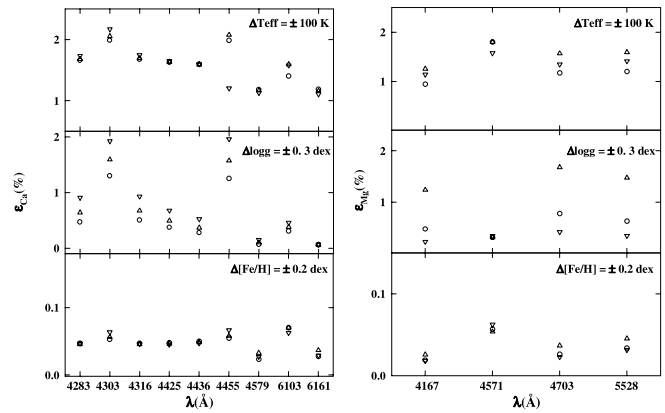
use LTE atmospheric models and perform our analysis just estimating non-LTE effects in statistical equilibrium.

3. NON-LTE CALCULATION AND RESULTS

To estimate Ca and Mg non-LTE abundances we used published equivalent widths (EWs) for 252 stars, including dwarfs, subdwarfs, and some subgiants. Sources of EW data are listed in Table 2 with the respective wavelengths of lines used in our analysis. Since we chose to work with one or two lines at maximum, we selected unsaturated and not very weak lines in order to have a more precise abundance determination.

To obtain non-LTE abundances we iterate MULTI with different abundance values until we reproduce the measured EW. This kind of procedure has two basic problems: (1) our atomic model is not perfect since, for example, we do not take into account all the levels and line transitions of all spectroscopic terms and certainly there are uncertainties in oscillator strengths and in collisional processes with neutral H and He (see TI99, for a discussion); and (2) there are observational errors in EW measurements and inhomogeneity of EWs from different sources (e.g., observations with

TABLE 2

SOURCES OF OBSERVED EW OF SELECTED LINES

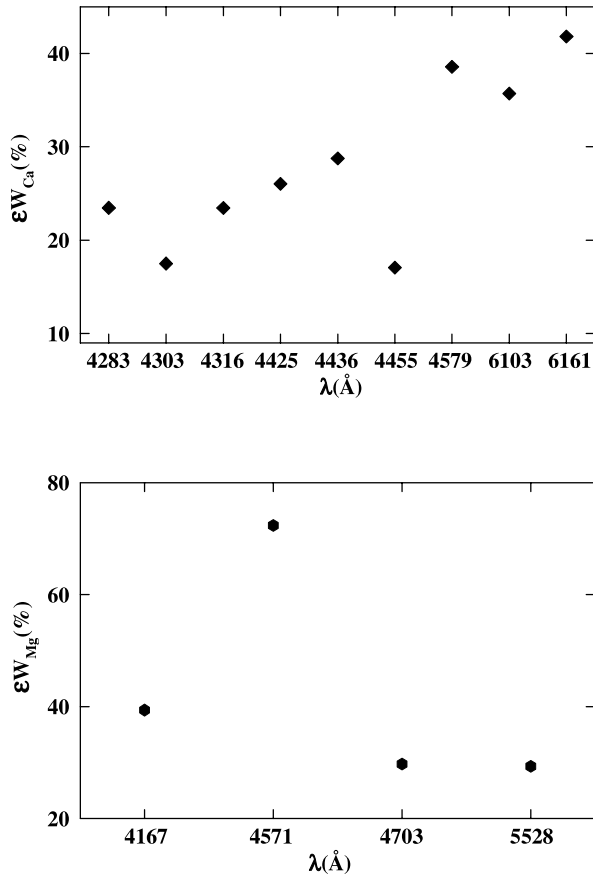| EW References	Ca I Lines (Å)	Mg I Lines (Å)
Edvardsson et al. 1993.................................	6166.44	8717.82
Nissen & Schuster 1997	6166.44	5711.1
Jehin et al. 1999	4578.56	4571.10
Zhao & Magain 1990.................................	4578.56	4571.1
Ryan, Norris, & Bessell 1991	4283.01, 4302.52	4167.27
	4318.65, 4454.78	...
Carney et al. 1997	6102.70	5528.42
Boesgaard et al. 1998	6161.30	4702.99
Peterson 1976, 1978, Peterson & Carney 1979......	4425.44, 4435.68	4571.10
Tomkin, Lambert, & Balachandran 1985	6166.44	8717.82
Perrin 1986...	4435.69	...
North, Berthet, & Lanz 1994	6717.69	...

FIG. 5.—Percentage errors in EW in function of variations of 0.15–0.2 dex in the abundance ratios [Ca/Fe] = +0.25 and [Mg/Fe] = +0.225 for the same lines as in Fig. 4.

FIG. 6.—Chemical abundance ratios in function of effective temperature ($\theta_{eff} = 5040/T_{eff}$). Different symbols follow the same legend as in Fig. 3.

different instruments and different placement of the continua).

In order to avoid systematic effects between EWs existing in the literature we renormalized our resulting abundances using common stars (comparison objects) present in the data sets of different authors. Of course, a standard procedure of renormalization requires a choice of comparison objects according to each spectral type of the analyzed stars. In our case this step was not necessary since our selected stars have roughly the same surface gravities (dwarfs and subgiants) and a narrow range of not very cool effective temperatures ($5300 < T_{eff} < 6300$).

All the stars were renormalized to a given reference system, to which we refer here as the Ed93 system (which is based on abundances derived from the published EW set of Edvardsson et al. 1993). First, we recalculate solar Ca, Mg, and Fe abundances using MULTI and EWs taken from Ed93. These values are our solar references. Then we estimate the relative abundances [Ca/H] and [Mg/H] for Ed93 stars. In principle, this differential procedure also allows us to minimize the imperfections of the atomic models used here. To renormalize the data from other sources we used observed common stars, as mentioned in the preceding paragraph. For example, for Mg abundance and mean metallicity $\langle[Fe/H]\rangle \approx -1$, to include the data of Jehin et al. (J99) into the Ed93 system, nine common stars between these two data sets were taken and the average of the differences between estimated abundances was calculated. This averaging procedure was used to transform J99 data to the
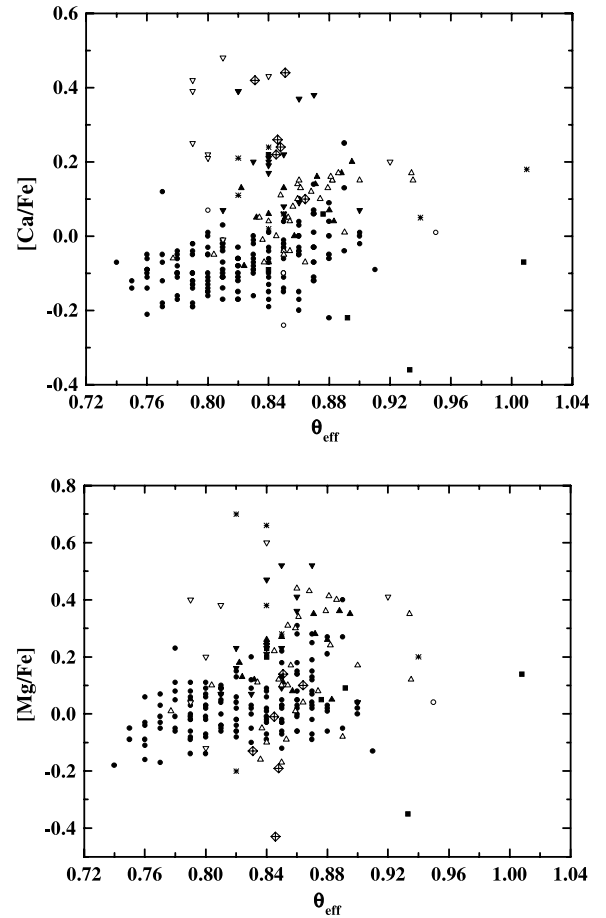
Ed93 system. The same procedure was performed on data given by Nissen & Schuster (NS97). For metal-poor stars more steps were performed. For the Zhao & Magain (ZM90) data, for example, we renormalized ZM90 into J99 (one common star) and ZM90 into NS97 (two common stars); then, as J99 and NS97 have common stars with the Ed93 system, these two sequences gave us a renormalization ZM90-Ed93.
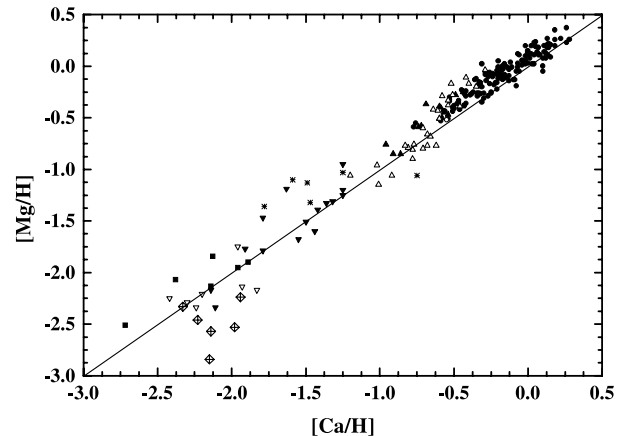

FIG. 7.—Relation between Mg and Ca abundances. Different symbols follow the same legend as in Fig. 3.

TABLE 3
NON-LTE ABUNDANCES FOR 252 STARS

Star	[Fe/H]$_{(NLTE)}$	[Ca/H]$_{(NLTE)}$	[Mg/H]$_{(NLTE)}$	EW Reference
BD +80 245	−1.78	−2.14	−2.13	C97
BD +20 3603	−2.04	−2.13	−1.84	C97
G 125-64	−2.16	−2.38	−2.07	C97
G 182-31	−2.18	−1.96	−1.95	C97
G 90-3	−1.95	−1.89	−1.90	C97
G 190-15	−2.65	−2.72	−2.51	C97
HD 400	−0.15	−0.26	−0.06	Ed93
HD 739	−0.02	0.1	−0.05	Ed93
HD 2454	−0.21	−0.32	−0.16	Ed93
HD 2615	−0.45	−0.42	−0.36	Ed93
HD 3158	0.08	0.04	0.02	Ed93
HD 3268	−0.13	−0.19	−0.09	Ed93
HD 4307	−0.17	−0.21	−0.22	Ed93
HD 5015	0.10	0.06	0.14	Ed93
HD 6434	−0.38	−0.32	−0.19	Ed93
HD 6920	−0.05	−0.17	−0.02	Ed93
HD 7439	−0.19	−0.29	−0.08	Ed93
HD 7476	−0.09	−0.28	−0.14	Ed93
HD 7570	0.18	0.12	0.13	Ed93
HD 9562	0.2	0.13	0.27	Ed93
HD 9826	0.08	−0.02	0.20	Ed93
HD 10307	0.08	−0.02	0.10	Ed93
HD 12042	−0.22	−0.25	−0.26	Ed93
HD 13555	−0.19	−0.21	−0.08	Ed93
HD 14214	0.15	0.07	...	Ed93
HD 15335	−0.08	−0.13	−0.14	Ed93
HD 15798	−0.10	−0.15	−0.11	Ed93
HD 16673	0.10	0.05	0.19	Ed93
HD 16895	0.08	−0.04	0.01	Ed93
HD 17548	−0.43	−0.46	−0.42	Ed93
HD 19994	0.18	0.13	0.18	Ed93
HD 20807	−0.05	−0.16	−0.08	Ed93
HD 22001	−0.01	−0.08	−0.19	Ed93
HD 22484	0.00	−0.07	−0.01	Ed93
HD 23754	0.16	0.04	0.11	Ed93
HD 25621	0.16	0.00	0.15	Ed93
HD 26491	−0.08	−0.08	−0.05	Ed93
HD 29645	0.16	−0.01	...	Ed93
HD 30562	0.22	0.22	0.27	Ed93
HD 30649	−0.40	−0.36	−0.13	Ed93
HD 30743	−0.21	−0.31	0.02	Ed93
HD 33256	−0.14	−0.31	...	Ed93
HD 33608	0.37	0.28	0.26	Ed93
HD 34411	0.09	−0.06	0.11	Ed93
HD 35296	0.10	8.88	0.18	Ed93
HD 38393	0.00	−0.02	0.06	Ed93
HD 41330	−0.07	−0.18	−0.09	Ed93
HD 43042	0.12	−0.06	−0.05	Ed93
HD 43318	−0.03	−0.17	−0.03	Ed93
HD 43947	−0.19	−0.22	−0.16	Ed93
HD 45701	0.20	0.13	0.11	Ed93
HD 48938	−0.26	−0.26	−0.17	Ed93
HD 49933	−0.27	−0.36	...	Ed93
HD 50223	−0.04	−0.09	−0.13	Ed93
HD 51530	−0.38	−0.53	−0.30	Ed93
HD 55575	−0.21	−0.25	−0.08	Ed93
HD 58551	−0.40	−0.43	−0.27	Ed93
HD 60532	−0.07	−0.13	−0.09	Ed93
HD 61421	0.05	−0.16	0.01	Ed93
HD 67228	0.14	0.02	0.12	Ed93
HD 68284	−0.41	−0.45	−0.23	Ed93
HD 68456	−0.15	−0.20	−0.08	Ed93
HD 69611	−0.40	−0.33	−0.15	Ed93
HD 69897	−0.12	−0.22	...	Ed93
HD 70110	0.12	0.1	0.00	Ed93
HD 74011	−0.46	−0.37	−0.25	Ed93

TABLE 3—*Continued*

Star	[Fe/H]$_{(NLTE)}$	[Ca/H]$_{(NLTE)}$	[Mg/H]$_{(NLTE)}$	EW Reference
HD 76151	0.10	−0.12	0.04	Ed93
HD 79028	0.00	−0.20	0.05	Ed93
HD 82328	−0.05	−0.10	−0.13	Ed93
HD 84737	0.15	0.08	0.11	Ed93
HD 86728	0.20	0.15	0.21	Ed93
HD 87141	0.15	−0.04	0.06	Ed93
HD 88737	0.26	0.11	0.20	Ed93
HD 88986	0.04	0.01	0.08	Ed93
HD 89125	−0.24	−0.34	...	Ed93
HD 89707	−0.28	−0.34	−0.26	Ed93
HD 89744	0.28	0.14	0.20	Ed93
HD 91752	−0.13	−0.23	...	Ed93
HD 91889	−0.11	−0.17	−0.13	Ed93
HD 95128	0.04	0.00	0.03	Ed93
HD 95241	−0.16	−0.21	−0.16	Ed93
HD 98553	−0.28	−0.30	−0.31	Ed93
HD 98991	0.00	−0.14	...	Ed93
HD 99747	−0.36	−0.42	...	Ed93
HD 102574......	0.22	0.13	0.19	Ed93
HD 102634......	0.30	0.14	0.20	Ed93
HD 102870......	0.22	0.10	0.08	Ed93
HD 106516......	−0.52	−0.53	−0.32	Ed93
HD 107113......	−0.35	−0.48	−0.36	Ed93
HD 107213......	0.36	0.18	0.35	Ed93
HD 108309......	0.15	0.12	0.08	Ed93
HD 108954......	0.00	−0.09	...	Ed93
HD 109358......	−0.05	−0.20	−0.12	Ed93
HD 110897......	−0.37	−0.42	−0.29	Ed93
HD 112164......	0.32	0.18	0.26	Ed93
HD 114642......	−0.05	−0.24	−0.07	Ed93
HD 114710......	0.15	−0.04	0.06	Ed93
HD 114762......	−0.56	−0.50	−0.41	Ed93
HD 114837......	−0.18	−0.21	−0.07	Ed93
HD 115383......	0.12	0.13	0.21	Ed93
HD 115617......	0.02	0.03	0.02	Ed93
HD 121370......	0.35	0.26	0.37	Ed93
HD 124570......	0.17	0.00	0.11	Ed93
HD 124850......	−0.05	−0.16	0.02	Ed93
HD 125184......	0.23	0.14	0.10	Ed93
HD 127334......	0.16	0.14	0.18	Ed93
HD 128167......	−0.29	−0.43	−0.38	Ed93
HD 128620......	0.20	0.14	0.22	Ed93
HD 130551......	−0.48	−0.50	−0.41	Ed93
HD 131117......	0.22	0.18	0.20	Ed93
HD 134169......	−0.71	−0.57	−0.43	Ed93
HD 136064......	0.10	−0.02	0.02	Ed93
HD 136351......	0.10	0.00	0.13	Ed93
HD 137052......	−0.05	−0.17	0.00	Ed93
HD 141004......	−0.01	−0.07	0.12	Ed93
HD 142373......	−0.27	−0.44	−0.24	Ed93
HD 142860......	−0.06	−0.21	−0.04	Ed93
HD 143761......	−0.12	−0.18	−0.04	Ed93
HD 144172......	−0.35	−0.34	−0.29	Ed93
HD 144585......	0.29	0.26	0.23	Ed93
HD 148211......	−0.47	8.88	−0.29	Ed93
HD 148816......	−0.51	−0.47	−0.36	Ed93
HD 150177......	−0.40	−0.51	−0.40	Ed93
HD 150453......	−0.23	−0.27	−0.29	Ed93
HD 151769......	0.15	−0.01	...	Ed93
HD 153597......	−0.04	−0.19	−0.06	Ed93
HD 155358......	−0.47	−0.47	−0.33	Ed93
HD 156098......	0.19	0.11	0.14	Ed93
HD 157089......	−0.39	−0.33	−0.26	Ed93
HD 157214......	−0.32	−0.19	−0.05	Ed93
HD 159307......	−0.54	−0.56	−0.44	Ed93
HD 159332......	−0.06	−0.19	−0.03	Ed93
HD 160032......	−0.16	−0.27	−0.10	Ed93

TABLE 3—*Continued*

Star	[Fe/H]$_{(NLTE)}$	[Ca/H]$_{(NLTE)}$	[Mg/H]$_{(NLTE)}$	EW Reference
HD 160933	−0.20	−0.23	−0.18	Ed93
HD 162396	−0.24	−0.31	...	Ed93
HD 163989	−0.05	−0.13	−0.03	Ed93
HD 165908	−0.40	−0.53	−0.34	Ed93
HD 168151	−0.19	−0.31	−0.20	Ed93
HD 169830	0.20	0.07	0.18	Ed93
HD 173667	−0.06	−0.06	...	Ed93
HD 174912	−0.42	−0.39	−0.28	Ed93
HD 175317	0.25	0.15	0.09	Ed93
HD 177565	0.07	0.07	0.11	Ed93
HD 181096	−0.13	−0.24	−0.10	Ed93
HD 184499	−0.59	−0.34	−0.19	Ed93
HD 187013	−0.06	−0.07	0.03	Ed93
HD 187691	0.18	0.07	0.12	Ed93
HD 193307	−0.22	−0.25	−0.25	Ed93
HD 196378	−0.30	−0.32	−0.27	Ed93
HD 198084	0.18	0.02	0.20	Ed93
HD 199289	−0.86	−0.76	−0.55	Ed93
HD 199623	−0.21	−0.31	−0.35	Ed93
HD 200790	0.03	−0.14	−0.01	Ed93
HD 201099	−0.39	−0.38	−0.27	Ed93
HD 201891	−0.87	−0.77	−0.59	Ed93
HD 205294	−0.21	−0.30	−0.26	Ed93
HD 207978	−0.45	−0.50	−0.38	Ed93
HD 208906	−0.58	−0.59	−0.53	Ed93
HD 210752	−0.47	−0.51	−0.44	Ed93
HD 210855	0.18	0.04	0.23	Ed93
HD 215257	−0.44	−0.54	−0.51	Ed93
HD 215648	−0.21	−0.29	−0.06	Ed93
HD 216385	−0.18	−0.35	−0.12	Ed93
HD 217014	0.16	0.05	0.24	Ed93
HD 218470	−0.04	−0.11	−0.01	Ed93
HD 218504	−0.46	−0.42	−0.24	Ed93
HD 222368	−0.10	−0.20	−0.01	Ed93
HD 59984	−0.62	−0.69	−0.37	J99
HD 61902	−0.59	−0.54	−0.47	J99
HD 63077	−0.66	−0.59	−0.40	J99
HD 63598	−0.73	−0.57	−0.45	J99
HD 78747	−0.61	−0.44	−0.25	J99
HD 79601	−0.53	−0.38	...	J99
HD 97320	−1.02	−0.96	−0.76	J99
HD 111971	−0.58	−0.58	−0.50	J99
HD 126793	−0.63	−0.49	−0.28	J99
HD 152924	−0.57	−0.44	−0.39	J99
HD 189558	−0.94	−0.74	−0.59	J99
HD 193901	−0.90	−0.86	−0.85	J99
HD 194598	−0.96	−0.91	−0.85	J99
HD 196892	−0.85	−0.72	−0.58	J99
HD 203608	−0.52	−0.60	−0.39	J99
M92-18	−2.45	−2.23	−2.46	B98
M92-21	−2.38	−2.14	−2.57	B98
M92-34	−2.43	−2.33	−2.33	B98
M92-46	−2.41	−2.15	−2.84	B98
M92-60	−2.40	−1.98	−2.53	B98
M92-350	−2.38	−1.94	−2.24	B98
BD +2 3375	−2.29	−1.91	−1.77	ZM90
BD +3 740	−2.50	−2.11	−2.34	ZM90
BD +17 4708	−1.54	−1.32	−1.31	ZM90
HD 16031	−1.56	−1.36	−1.33	ZM90
HD 19445	−1.88	−1.79	−1.47	ZM90
HD 34328	−1.42	−1.25	−0.95	ZM90
HD 59392	−1.44	−1.25	−1.20	ZM90
HD 74000	−1.83	−1.44	−1.60	ZM90
HD 84937	−1.86	−1.79	−1.79	ZM90
HD 116064	−1.87	−1.50	−1.51	ZM90
HD 140283	−2.21	−2.14	−2.17	ZM90
HD 160617	−1.48	−1.42	−1.39	ZM90

TABLE 3—*Continued*

Star	[Fe/H]$_{(NLTE)}$	[Ca/H]$_{(NLTE)}$	[Mg/H]$_{(NLTE)}$	EW Reference
HD 166913	−1.46	−1.25	−1.25	ZM90
HD 181743	−1.71	−1.63	−1.19	ZM90
HD 213657	−1.75	−1.55	−1.68	ZM90
BD −21 3420	−0.88	−0.77	−0.76	NS97
CD −33 3337	−1.16	−1.2	−1.06	NS97
CD −45 3283	−0.72	−0.71	−0.80	NS97
CD −47 1087	−0.64	−0.51	−0.28	NS97
CD −57 1633	−0.73	−0.78	−0.90	NS97
CD −61 0282	−0.97	−0.92	−1.06	NS97
G 005-040	−0.68	−0.54	−0.38	NS97
G 046-031	−0.61	−0.68	−0.66	NS97
G 088-040	−0.64	−0.64	−0.42	NS97
G 102-020	−0.93	−0.78	−0.81	NS97
HD 3567	−1.05	−1.01	−1.15	NS97
HD 17288	−0.75	−0.6	−0.51	NS97
HD 17820	−0.54	−0.42	−0.11	NS97
HD 22879	−0.67	−0.54	−0.33	NS97
HD 24339	−0.48	−0.52	−0.17	NS97
HD 25704	−0.68	−0.60	−0.51	NS97
HD 76932	−0.73	−0.58	−0.29	NS97
HD 83220	−0.40	−0.46	−0.39	NS97
HD 103723	−0.61	−0.62	−0.77	NS97
HD 105004	−0.64	−0.71	−0.60	NS97
HD 106038	−1.07	−1.02	−0.96	NS97
HD 113083a	−0.78	−0.68	−0.77	NS97
HD 113083b	−0.76	−0.66	−0.68	NS97
HD 113679	−0.45	−0.29	−0.037	NS97
HD 120559	−0.78	−0.61	−0.43	NS97
HD 121004	−0.57	−0.40	−0.17	NS97
HD 126681	−0.96	−0.81	−0.79	NS97
HD 241253	−0.87	−0.83	−0.77	NS97
W7547	−0.30	−0.35	−0.20	NS97
HD 48565	−0.54	−0.64	…	North
HD 147609	−0.36	−0.29	…	North
HD 99383	−1.36	−1.60	…	Per86
BD +26 3578	−2.02	−1.78	−1.36	Pet76
BD +34 2476	−1.80	−1.59	−1.10	Pet78
HD 64090	−1.52	−1.47	−1.32	Pet78
HD 94028	−1.31	−1.25	−1.03	Pet78
HD 97916	−0.86	−0.75	−1.06	Pet78
HD 108177	−1.51	−1.49	−1.13	Pet78
HD 103095	−1.19	−1.01	…	Pet79
BD −33 1173	−2.69	−2.3	−2.29	R91
BD −13 3442	−2.72	−2.24	−2.34	R91
CD −71 1234	−2.05	−1.83	−2.17	R91
L56-75	−2.41	−2.20	−2.21	R91
L635-14	−2.18	−1.93	−2.14	R91
L732-48	−2.08	−2.09	…	R91
L815-43	−2.64	−2.22	…	R91
L831-70	−2.85	−2.42	−2.25	R91
LR 740	−2.16	−1.96	−1.75	R91
HD 6582	−0.56	−0.55	−0.52	Tom85
Sun	0	0	0	…

REFERENCES.—(C97) Carney et al. 1997; (Ed93) Edvardsson et al. 1993; (J99) Jehin et al. 1999; (B98) Boesgaard et al. 1998; (ZM90) Zhao & Magain 1990; (NS97) Nissen & Schuster 1997; (North) North et al. 1994; (Per86) Perrin 1986; (Pet76) Peterson 1976; (Pet78) Peterson 1978; (Pet79) Peterson & Carney 1979; (R91) Ryan et al. 1991; (Tom85) Tomkin et al. 1985.

The main goal of this procedure is to have a homogeneous table of derived non-LTE abundances. Results are presented in Table 3 for Ca and Mg. Figure 3 shows the abundance ratios [Ca/Fe] and [Mg/Fe] for halo and disk phases, presenting parallel structures in both evolutive diagrams.

Errors are hard to estimate because they involve many factors, as described previously. We estimated the uncertainties in our abundance determinations caused by the scatter on derived abundances when varying different parameters: stellar (T_{eff}, log g, and [Fe/H]) and observational (EW). Figure 4 shows the percentage errors on log (N_{Ca}) and log (N_{Mg}) abundances, corresponding to an incertitude in a given atmospheric parameter. These error estimates are made for a star of $\theta_{eff} = 0.85$, log $g = 4.2$, and [Fe/H] $= -2.0$, for different abundance ratios [Ca/Fe] and [Mg/Fe], for the Ca I and Mg I lines of Table 2. We see that abundance variations are, on the average, more sensitive to uncertainties in T_{eff}, reaching a maximum of 2.2% for some Ca I lines. We note that, in the case of log g and [Fe/H], the scatters adopted are the classical LTE errors, so the abundance errors can be overestimated.

A similar analysis is made for EW uncertainties using the same Ca I and Mg I lines. Figure 5 shows the percentage errors in EW if we have errors in abundance ratios of the order of the structure separations (≈ 0.15, 0.2 dex in the halo phase) displayed in Figure 3. For example, the EWs of Ca I 4578.56 Å and Mg I 4571.1 Å lines from Zhao & Magain 1990 have, respectively, errors of 40% and 75% when [Ca/Fe] and [Mg/Fe] have variations between 0.15 and 0.2 dex. The magnitudes of these uncertainties are much greater than the observational errors estimated by EW sources, demonstrating that these structures can be real.

Figure 3 confirms that effects of data renormalization as sources of these structures can be discarded since the data of distinct sources are distributed in different parallel structures. As mentioned above, scattering in abundances is sensitive to temperature variations; however, this effect seems to be not strong enough to form these structures, as can be seen in Figure 6, which shows no correlation between abundance ratios and temperatures.

One should also keep in mind that such uncertainties in T_{eff} or log g result in variations in iron abundances of the same magnitude and sign as for Ca and Mg abundances, which minimizes uncertainties in the abundance ratios. Thus, one can say that the ratios [Ca/Fe] and [Mg/Fe] are less sensitive to these uncertainties on the stellar fundamental parameters.

4. DISCUSSION

The two non-LTE chemical diagrams in Figure 3 show that the chemical enrichment of the matter in our Galaxy may not be as simple as currently accepted. On the [Ca/Fe] diagram, parallel structures appear: (1) the halo phase shows three well-defined structures separated by ≈ 0.15 dex and some very Ca-deficient stars, and (2) in the disk phase ($-0.7 <$ [Fe/H] < 0.4) one can distinguish at least four structures. This behavior is also present in the intermediate phase of the Galaxy ($-1.2 <$ [Fe/H] < -0.7) but only on three incurved structures.

The [Mg/Fe] diagram shows the same structures but with a greater scatter. This scatter could be essentially the result of two facts: first, measured EWs for magnesium lines are more imprecise (there are fewer clean weak

lines in observed spectra) than for calcium lines, and second, there are some differences between the mechanisms of Mg and Ca yield production by SNe II of distinct progenitor masses. Figure 7 shows a pronounced scatter in the [Mg/H] and [Ca/H] relation in the halo phase.

Clearly, the structures pointed out by Nissen & Schuster (1997) and Jehin et al. (1999) are present in our calcium and magnesium diagrams and now extend to the disk and halo phases of our Galaxy. Flat structures of [α/H] ratios versus [Fe/H] are consistent with the idea that both elements come from massive supernovae. The question is how field star formation can produce these structures if, at first, halo stars were formed independently throughout the entire protogalaxy.

Such structures and dichotomy also exist in globular clusters, as has been demonstrated more than 15 years ago. Calcium branch dichotomy in ω Cen revealed possible self-enrichment due to SNe II, suggesting two epochs of star formation separated by a hiatus. Detailed discussion by Norris, Freeman, & Mighell (1996) rejects with convincing arguments a merger origin of the dichotomy of [Ca/H] abundances in globular clusters. Another intriguing coincidence is the bimodality of C and N abundances on the main sequence of 47 Tuc (Cannon et al. 1998). As suggested by the authors, a hybrid accretion-enrichment model could help to explain how globular clusters form and the role played by stellar winds and those of SNe II. Recently Boesgaard et al. (1998) have observed six turnoff stars in M92, an old very metal-poor cluster. Keeping in mind that the quality of the spectra is low, producing large uncertainties in possible derived chemical abundances from them, we derived non-LTE abundances for iron, calcium, and magnesium. As an exercise, we plotted the Ca and Mg ratios for these six stars on our diagram and discovered after renormalization that they lie at exactly the same places as for halo stars. To conclude that this is more than a coincidence is premature but raises an interesting possibility: a common origin for field and globular cluster stars. If such observations could be repeated in other globular clusters for main-sequence stars with better signal-to-noise ratios (S/Ns), then they would probably help greatly in the understanding of the formation of the Galaxy. Possible consequences could also be derived concerning the first stars in the protogalaxy as discussed by Cayrel (1986).

Another possible scenario of the formation of the Galaxy that can produce these structures in the halo phase is an incomplete mixing of SN II yields, as suggested by Karlsson & Gustafsson (2000). In an even more recent paper, Argast et al. (1999) have explored this scenario in more detail. Surprisingly, the model proposed by Argast et al. produces structures in the [Ca/Fe] and [Mg/Fe] diagrams ([Fe/H] < -1.5) similar to ours, as shown in Figure 3. Their theoretical [Mg/Fe] diagram also shows greater scatter than the [Ca/Fe] diagram, suggesting that the origin of this difference is mainly the yield production mechanism (see Argast et al. 1999 for more details), as mentioned in the second paragraph of this section.

For the disk phase, observed structures have a smaller separation and are more evident in the [Ca/Fe] diagram than in the [Mg/Fe] diagram. One interesting question is how can chemical evolution models reproduce this result for disk metal-rich stars? Is it that the mixing timescale of enriched gas was larger than the formation time of each generation of stars in the disk, as supposed for the halo

phase? Observations of open cluster stars could verify whether they have similar behavior to globular cluster stars.

5. CONCLUSIONS

We report here non-LTE differential abundances for 252 subdwarf to subgiant stars using published high-resolution equivalent widths. [Ca/Fe] and [Mg/Fe] diagrams show remarkable structures in both the halo and disk phases of the Galaxy, which are not related to observational or atmospheric parameter uncertainties. These results lead us to a possible evolutive galactic scenario of nonhomogeneity or incomplete mixing of synthesized SN II yields (Karlsson & Gustafsson 2000; Argast et al. 1999). A surprising result is the behavior of M92 stars, mainly in the Ca diagram, suggesting a common origin for field and cluster stars. Spectroscopic high resolution with good S/N of stars in clusters is

needed to confirm or refute the sketch of a new chemical evolution model presented in this work. New non-LTE analysis for other α-elements is also necessary to verify whether this structural behavior applies to all α-capture SN II products.

REFERENCES

Argast, D., Samland, M., Gerhard, O. E., & Thielemann, E.-K. 1999, preprint (astro-ph/9911178)
Audouze, J., & Silk, J. 1995, ApJ, 451, L49
Baumuller, D., & Gehren, T. 1997, A&A, 325, 1088
Bell, R. A., Eriksson, K., Gustafsson, B., & Nordlund, A. 1976, A&AS, 23, 37
Belyakova, E. V., & Manshonkina, L. I. 1997, Astron. Rep., 41, 530
Boesgaard, A. M., Deliyannis, C. P., Stephens, A., & King, J. R. 1998, ApJ, 493, 206 (B98)
Cannon, R. D., Croke, B. F. W., Bell, R. A., Hesser, J. E., & Stathakis, R. A. 1998, MNRAS, 298, 601
Carlsson, M. 1986, Uppsala Astron. Obs. Rep., 33
Carney, B. W., Wright, J. S., Sneden, C., Laird, J. B., Aguilar, L. A., & Latham, D. W. 1997, AJ, 114, 363 (C97)
Cayrel, R. 1986, A&A, 168, 81
Cayrel, R., Faurobert-Scholl, M., Feautrier, N., Spielfiedel, A., & Thévenin, F. 1996, A&A, 312, 549
Drake, J. J. 1991, MNRAS, 251, 369
Edvardsson, B., Andersen, J., Gustafsson, B., Lambert, D., Nissen, P., & Tomkin, J. 1993, A&AS, 102, 603 (Ed93)
Gigas, D. 1986, A&A, 165, 170
———. 1988, A&A, 192, 264
Gustafsson, B., Bell, R. A., Eriksson, K., & Nordlund, A. 1975, A&A, 42, 407
Hirata, R., & Horaguchi, T. 1995, Catalogue of Atomic Spectroscopic Lines, Vol. 6 (Strasbourg: CDS), 69 (HH95)
Jehin, E., Magain, P., Neuforge, C., Noels, A., Parmentier, G., & Thoul, A. A. 1999, A&A, 341, 241 (J99)
Karlsson, T., & Gustafsson, B. 2000, in Colloq. 35, The Galactic Halo: from Globular Clusters to Field Stars (Liège: Univ. Liège Press), in press

Kiselman, D., & Carlsson, M. 1996, A&A, 311, 680
Kurucz, R. L. 1993, Kurucz CD-ROM 8, Kurucz Atomic Data Files (Cambridge: SAO)
Mashonkina, L. I., & Bikmaev, I. F. 1996, Astron. Rep., 40, 94
Mashonkina, L. I., Sakhibullin, N. A., & Shimanskii, V. V. 1993, Astron. Rep., 37, 192
Mashonkina, L. I., Shimanskaya, N. N., & Sakhibullin, N. A. 1996, Astron. Rep., 40, 187
Martin, W. C., Kaufman, V., Zalubas, R., Musgrove, A., Sugar, J., & Corliss, C. 1985, J. Phys. Chem. Ref. Data, 10, 195
Mishenina, T. V., Korotin, S. A., Klochkova, V. G., & Panchuk, V. E. 2000, A&A, 353, 978
Nissen, P., & Schuster, W. J. 1997, A&A, 326, 751 (NS97)
Norris, J. E., Freeman, K. C., & Mighell, K. J. 1996, ApJ, 462, 241
North, P., Berthet, S., & Lanz, T. 1994, A&AS, 103, 321 (North)
Perrin, M. N. 1986, A&A, 159, 239 (Per86)
Peterson, R. 1976, ApJ, 206, 800 (Pet76)
———. 1978, ApJ, 222, 181 (Pet78)
Peterson, R., & Carney, B. 1979, ApJ, 231, 762 (Pet79)
Ryan, S. G., Norris, J. E., & Bessell, M. S. 1991, AJ, 102, 303 (R91)
Thévenin, F. 1989, A&AS, 77, 137
———. 1990, A&AS, 82, 179
———. 1998, Bull. CDS 49, Catalogue III/193
Thévenin, F., & Idiart, T. 1999, ApJ, 521, 753 (TI99)
Tomkin, J., Lambert, D., & Balachandran, S. 1985, ApJ, 290, 289
Unsöld, A. 1955, Physik der Sternatmospheren (Berlin: Springer)
Zhao, G., Butler, K., & Gehren, T. 1998, A&A, 333, 219
Zhao, G., & Magain, P. 1990, A&AS, 86, 85 (ZM90)